ACS APPLIED MATERIALS & INTERFACES

Research Article

www.acsami.org

Highly Efficient and Low Turn-On Voltage Quantum Dot Light-Emitting Diodes by Using a Stepwise Hole-Transport Layer

Wenyu Ji,*[,†] Ying Lv,[†] Pengtao Jing,[†] Han Zhang,[‡] Jia Wang,[†,‡] Hanzhuang Zhang,*[,‡] and Jialong Zhao*[,§]

[†]State Key Laboratory of Luminescence and Applications, Changchun Institute of Optics, Fine Mechanics and Physics, Chinese Academy of Sciences, Changchun 130033, China

[‡]Department of Physics, Jilin University, Changchun 130012, China

[§]Key Laboratory of Functional Materials Physics and Chemistry of the Ministry of Education, Jilin Normal University, Siping 136000, China

Supporting Information

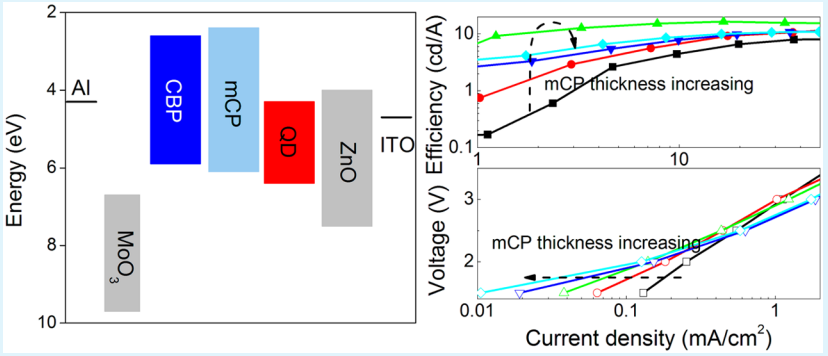

ABSTRACT: Highly efficient red quantum dot light-emitting diodes (QD-LEDs) with a very high current efficiency of 16 cd/A were demonstrated by adopting stepwise hole-transport layers (HTLs) consisting of 4,4′-*N*,*N*′-dicarbazole-biphenyl (CBP) combined with *N*,*N*′-dicarbazolyl-3,5-benzene (mCP). The mCP layer plays two important roles in this kind of QD-LEDs. One is that it can block the electron to leak into the HTL due to its higher LUMO (LUMO = the lowest unoccupied molecular orbital) energy level than that of CBP; and the other is it can separate the carrier accumulation zone from the exciton formation interface, which is attributed to the stepwise hole-transport layer structure. Moreover, the lower HOMO (HOMO = the highest occupied molecular orbital) energy level of mCP decreases the hole-injection barrier from the HTL to the QD emitting layer, which improves the charge carrier balance injected into the QD layer, reducing the turn-on voltage of QD-LEDs fabricated with the stepwise HTL structure.

KEYWORDS: *quantum dots, light emitting diodes, stepwise hole-injection layer, leakage current, charge accumulation*

INTRODUCTION

Colloidal quantum dots (QDs) have attracted much attention due to their many advantages over their organic/polymer counterparts, including narrow emission bands, a broad wavelength tunability from UV to infrared through the size and/or composition variation(s), good photostability, and low-cost wet chemical processing technology.[1−16] All these attractive characteristics make QDs excellent candidates as the emitters for the next-generation display and lighting technologies. The QD materials have already entered the display and lighting market offering enhanced color purity as the down-conversion unit combined with backlighting inorganic LEDs. Moreover, QD-based light emitting diodes (QD-LEDs) demonstrated about three decades ago are still in the research and development stage,[2] but there has been great progress in enhancing the device performances, closing to that of organic LEDs,[16,17] which have been intensely investigated for at least two decades.[18,19] The external quantum efficiency has been increased from less than 0.01% to over 20%.[2,17] Recently, the most efficient performance of QD-LEDs with an EQE of 20.5% was reported by the Peng group benefiting from the inorganic ZnO nanoparticle electron transport layer (ETL) combined with organic hole transport layers (HTLs).[17] The ZnO ETL has high electron mobility, matched conduction energy level with QDs, and good stability, which are required to fabricate efficient QD-LEDs. To date, the ZnO nanoparticle film has been demonstrated as the best candidate as the ETL in QD-LEDs and very highly efficient QD-LEDs have been fabricated.[8−10,12,14,15,17] The effect of the ZnO/QDs interface on the device performance has been investigated in detail, and device efficiency is enhanced by introducing an insulating poly(methyl methacrylate) layer to suppress the exciton

Received: May 10, 2015
Accepted: July 3, 2015
Published: July 3, 2015

DOI: 10.1021/acsami.5b04050
ACS Appl. Mater. Interfaces 2015, 7, 15955−15960

quenching induced by ZnO.[17] Moreover, light emission at sub-bandgap driving voltage has also been observed due to efficient electron injection from ZnO to QDs.[9,16,17,20,21] However, the overall performance of QD-LEDs is currently lagging behind their organic counterpart, and there is still large room to further improve the device performance. Considering the fact that efficient electron injection and interface engineering have been achieved for the ZnO ETL, one alternative strategy to enhance device performance is optimizing HTL to simultaneously achieve efficient hole injection and exciton confinement in the QD emission layer. With regard to hole transport, it is well-known that a large injection barrier exists between the HTL and QD layer in QD-LEDs. Improved carrier injection and confinement are essential in order to improve the QD-LED performance. Thereby, it is desirable for a hole transport material having high LUMO and low HOMO energy level simultaneously, which can block the electron to diffuse into HTL and enhance the hole injection from HTL to QDs. In other words, a wide band gap hole transport material is necessary for efficient QD-LEDs. Various processes have been proposed to form the HTL, including phase separation,[20] thermal polymerization, and evaporation.[23] However, how to design a highly efficient HTL structure is still a major challenge in the conventional QD-LEDs due to the limitation of solution technology, in which the underlying solvent-sensitive organic layers are inevitably damaged to a certain extent to achieve a multilayer device structure even though orthogonal solvents are used. In addition, most of the reported QD-LEDs suffer from unbalanced charge transport due to the misalignment between the extremely low valence band edge of QDs against the HOMOs of organic HTLs and lower hole mobility of polymer hole transport materials than that of ZnO nanoparticle ETL. It is desirable to systematically manage the HTLs and HTL/QDs interface to enhance the device performance. Fortunately, it is very flexible to engineer the HTL with an inverted device structure,[8−10,24] in which the indium tin oxide (ITO) is used as the cathode and solution processed ZnO film as the ETL and the HTLs are deposited by thermal evaporation technique. In contrast to the solution spin-coating processes that can destroy the underlying organic HTLs when depositing the QDs layer in the conventional devices, the thermally evaporation technique almost never damages the underlayers in the inverted structure devices. Moreover, it is very easy to construct a multilayer HTL structure to improve the device performance by the thermal evaporation technology.

In this work, we for the first time introduce *N*,*N*′-dicarbazolyl-3,5-benzene (mCP) into the inverted QD-LEDs as both HTL and electron blocking layer (EBL). Compared with the commonly used 4,4′-*N*,*N*′-dicarbazole-biphenyl (CBP) HTL, the mCP possesses higher LUMO and lower HOMO energy level, which improves the hole injection and charge carrier confinement in QDs and enhances the performance of QD-LEDs. In addition, the bilayer HTL composed of CBP and mCP forms a stepwise structure for the hole injection/transport and suppressing the exciton quenching induced by the accumulated holes at the HTL/QDs interface. The peak current efficiency of the QD-LEDs with the stepwise HTL is 16 cd/A, which is about 100% higher than that of the CBP only device.

EXPERIMENTAL DETAILS

According to the device structure shown in Figure 1a, all QD-LEDs were built on the indium tin oxide (ITO) coated glass

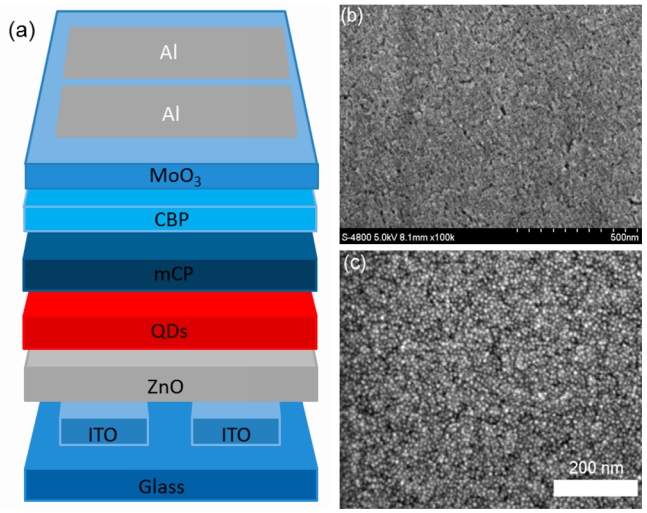

Figure 1. (a) Schematic structure of the device; SEM images of (b) ZnO NPs on ITO substrate and (c) CdSe/ZnS QDs on ZnO/ITO substrate.

substrates with a square resistance of 12 Ω/square. All the substrates were ultrasonically cleaned in acetone, ethanol, deionized water, and isopropanol in sequence and followed by an ex situ UV ozone treatment in air for 5 min. The ZnO nanoparticles were deposited onto the cleaned and UV ozone treated ITO substrates by spin-coating process from a 30 mg/mL ZnO butanol solution and then annealed at 120 °C for 30 min in a glovebox (MBRAUN). Afterward, the QDs were spin-coated onto a ZnO layer from QD toluene solution (5 mg/mL) at 2000 rpm and then annealed at 70 °C for 30 min in the same glovebox (MBRAUN). The thicknesses of ZnO and QD are around 45 and 30 nm, respectively, determined by SEM measurements. Finally, the HTL of mCP (*x* nm)/CBP (60-*x* nm), hole injection layer of MoO_3 (5 nm), and anode of Al (100 nm) was thermally evaporated in high vacuum at pressure below 4×10^{-6} Torr. Five different QD-LEDs were fabricated with different thicknesses of mCP layer, Device A (0 nm), Device B (5 nm), Device C (10 nm), Device D (30 nm), and Device E (60 nm), while the total thickness of the HTL of mCP/CBP remains the same for all the devices. The Al cathode lines with a width of 2.5 mm were deposited orthogonally to the ITO anode lines, and a 5 mm^2 active area was formed. The ZnO nanoparticles and red CdSe/ZnS core−shell QDs were synthesized with a method in previous reports.[8,25] The CBP and mCP were purchased from LumTec and were used as received without any further purification.

Detailed measurement processes for QD-LEDs have been described in our previous papers.[26] The spectra of the devices were measured with an Ocean Optics Maya 2000-PRO spectrometer. The room temperature absorption spectrum was measured with an ultraviolet/visible spectrometer (UV 1700, Shimadzu), and the PL spectrum was collected by a Hitachi F-4500 spectrophotometer under an excitation wavelength of 400 nm. Note that the absorption and PL spectra were obtained from the QD toluene solution. The transmission electron microscopy (TEM) images were recorded on a Philips TECNAI G2, and scanning electron microscopic (SEM) images were measured with by a Hitachi S4800. HOMO levels of CBP and mCP were obtained from cyclic voltammetry measurements, and the results are shown in Figure S1 in the Supporting Information. The cyclic voltammetry measurements

DOI: 10.1021/acsami.5b04050
ACS Appl. Mater. Interfaces 2015, 7, 15955−15960

were performed on CHI 920C electrochemical workstation (Shanghai Chenhua). Atomic force microscopy (AFM) images were recorded in the tapping mode by Bruker Multimode-8.

RESULTS AND DISCUSSION

Red CdSe/ZnS based inverted QD-LEDs were fabricated with the typical device scheme via solution and thermal evaporation processes for the constituent layers as shown in Figure 1a. The ZnO nanoparticles with a diameter of 3−5 nm and photoluminescence (PL) peak at 530 nm as shown in Figures S2 and S3 in the Supporting Information were synthesized according to the method reported previously.[8] The morphologies of ZnO and QD layers were characterized by SEM measurements as shown in Figure 1b,c, respectively. A homogeneous ZnO film on ITO substrate was observed from the SEM image. Moreover, the ZnO film possesses a moderate surface roughness as characterized by AFM measurement. The root-mean-square (RMS) of the ZnO layer is 5.3 nm as shown in the Figure S4 in the Supporting Information. With optimized deposition conditions, relatively uniform and compactly packed QD layers were also obtained on ZnO film, which could effectively reduce the leakage current induced by the incomplete cover of ZnO layer by QDs and ensures the fabrication of highly efficient QD-LEDs. Figure 2a is the absorption and PL spectra of QDs in toluene, as well as the PL spectrum of QD film. As can be seen, the PL peak of the QD film shows a redshift compared with that of QDs in toluene. This is likely due to the Förster resonant energy transfer from smaller QDs (donor) to the larger one (acceptor) within the film. In addition, note that the exciton absorption peaks are not distinct as shown in Figure 2a, which is due to an alloy interface in CdSe/ZnS QDs. The TEM image of QDs is shown in Figure 2b, and we can see uniform and monodisperse QDs were synthesized with a diameter of around 8 nm. The high resolution TEM image shown in the inset of Figure 2b exhibits that no distinct boundary exists between the core and shell, which is attributed to the continuous composition gradient and alloy transition interface inside the QDs and is well in agreement with the absorption results depicted in Figure 2a.

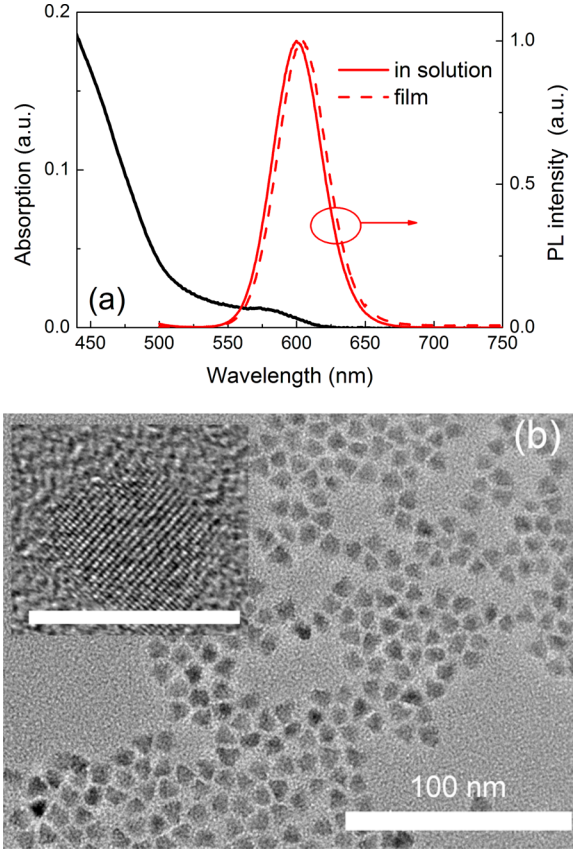

Figure 2. (a) Absorption and PL spectra and (b) the TEM image of the CdSe/ZnS core/shell QDs. Inset in (b) is the high resolution TEM image of QDs, and the scale bar is 10 nm.

Small molecule material of mCP, having higher triplet energy and larger band gap, i.e., lower HOMO and higher LUMO energy level, than that of CBP, is a widely used host and/or HTL in organic LEDs. Herein, we for the first time introduce mCP into the inverted QD-LEDs due to its outstanding properties. Figure 3a shows the current density−voltage characteristics of QD-LEDs with and without mCP. We can see that the current density of the devices with mCP is lower than that of device A with single CBP as the HTL in the range of operation voltages is lower than 2.5 V; the thicker mCP, the lower current density. The phenomenon can be explained by the schematic energy level diagram shown in Figure 3b. As can be seen, the LUMO energy level of mCP is 0.2 eV higher than that of CBP, which decreases the leakage of electrons into the HTL, benefiting to the efficiency in the QD-LEDs. In addition, we also observe that the current density of mCP-containing devices is higher than that of a device with single CBP as the HTL at high operation voltage region, which may be due to the

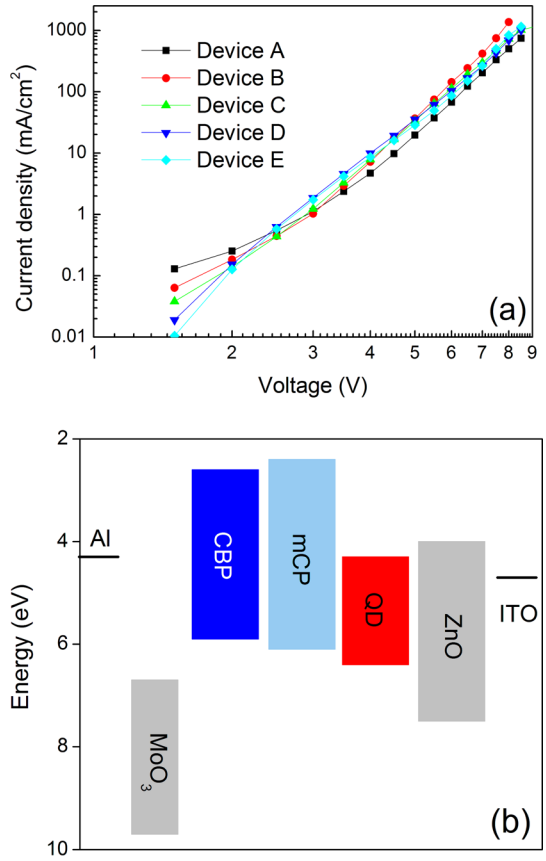

Figure 3. (a) Current density−voltage characteristics of all the QD-LEDs; (b) flat energy level diagram of the materials used in this study.

DOI: 10.1021/acsami.5b04050
ACS Appl. Mater. Interfaces 2015, 7, 15955−15960

smaller hole injection barrier between HTL and QDs when the mCP is inserted into the CBP/QD interface. Similar phenomena were also reported previously,[27] where the introduction of a low hole mobility CBP:MoO_3 ($\sim 10^{-6}$ cm^2 V^{-1} s^{-1}) layer dramatically enhanced the device current density due to the lower hole injection barrier. In our QD-LEDs, a p-doping but not pristine MoO_3 layer will be formed as a so thin (5 nm) MoO_3 was deposited on the CBP layer, which improves the hole injection from Al anode to CBP. In addition, it is worthy to note that the effect of mCP thickness on the current density at the range of high operation voltage is not very obvious due to the similar hole mobility of 0.5×10^{-3} and 1×10^{-3} cm^2 V^{-1} s^{-1} for mCP[28] and CBP[8], respectively. However, the small variation of holes current in the HTL still affects the device efficiency significantly induced by the carrier balance condition due to the slightly lower hole mobility of mCP than the electron mobility of ZnO (10^{-3} cm^2 V^{-1} s^{-1})[8] (we will discuss these in Figure 4b).

The luminance−voltage curves of QD-LEDs are shown in Figure 4a. We can see that the device luminance is enhanced dramatically as the mCP introduced into the devices in all the operation voltage range. For example, the luminances are 776, 1984, 2563, 2129, and 1754 cd/m^2 for devices A, B, C, D, and E, respectively, at the operation voltage of 5 V. The luminance of all the mCP-containing devices is similar but higher than that of CBP based device, which is attributed to both blocking of electron and improved hole injection in QDs by the mCP layer, in spite of its hole mobility being slight lower than that of CBP. Another interesting aspect is the device turn-on voltage (herein the turn-on voltage is defined as the applied voltage when the device luminance is 1 cd/m^2) is decreased with the mCP insertion, around 2.1 and 2.4 V for devices with and without mCP layer, respectively. This enhancement is attributed to the enhanced hole injection from mCP into the QDs due to the decreased hole injection barrier. The detailed performance of all the QD-LEDs is listed in Table 1. Figure 4b shows the current−density efficiency characteristics of the QD-LEDs, and the optimized thickness of mCP is 10 nm considering the device efficiency. Further increasing the mCP thickness decreases the device efficiency, which is attributed to the slightly lower hole mobility of mCP than that of CBP. However, we can see that device efficiency of mCP-containing QD-LEDs is higher than the control device with single CBP as the HTL. We contribute the enhancement to the limitation of electron diffusion from QDs to HTL due to the large barrier between the conduction band of QDs and the LUMO energy level mCP, which suppresses the leakage current in QD-LEDs. The correlation between the current efficiency and turn-on voltages of devices versus mCP thickness indicates that the energy level alignment for HTL and QDs plays a more important role than the charge mobility in the device performance, and similar results were also reported by other groups.[8,29,30] It can be anticipated that the performance of QD-LEDs will be further improved when an HTL with higher mobility and more matched energy level is adopted. In addition, an encouraging high reproducibility of this high performance of our QD-LEDs was demonstrated by testing 69 devices from 5 batches as shown by the histograms in Figure 4c, yielding an average efficiency of 15.6 cd/A. The good reproducibility of the devices is benefited from the high film quality of QD, ZnO, and organic layers and stability of QDs.

Figure 5 depicts the electroluminescence (EL) spectra of QD-LEDs at a driving voltage of 5 V together with photographs

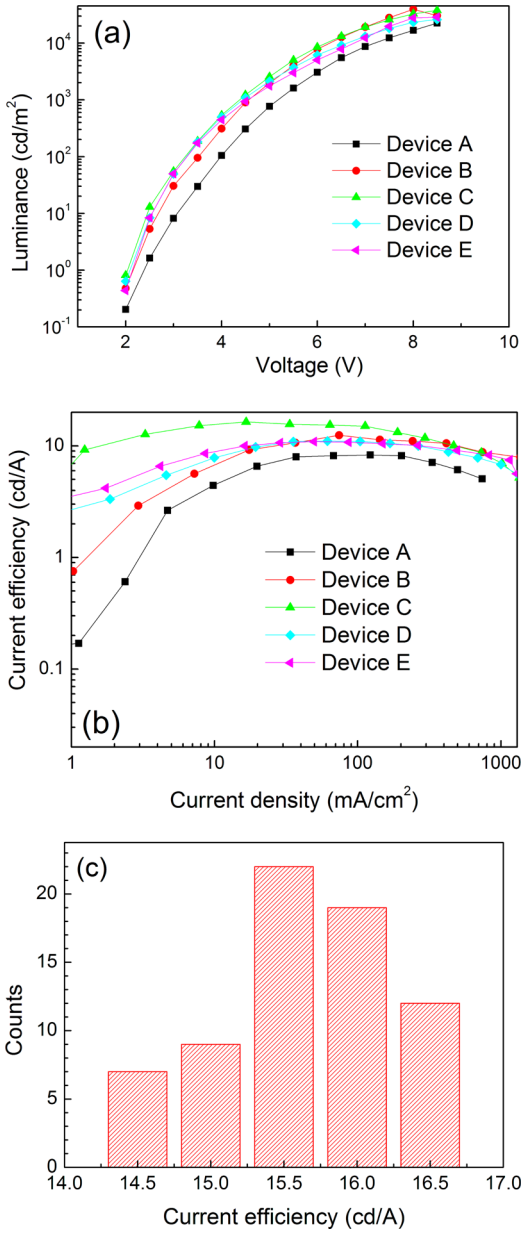

Figure 4. (a) Voltage−luminance and (b) efficiency−current density curves of all the devices; (c) histogram of current efficiencies measured from 69 devices. The average current efficiency is 15.6 cd/A.

Table 1. Summary of the Performance of QD-LEDs[a]

device	L_{max} (cd/m^2)	η_{max} (cd/A)	V_T (V)
A	22488	8.3	2.38
B	39490	12.5	2.15
C	37850	16.5	2.04
D	26140	11.0	2.08
E	28750	10.9	2.13

[a] L_{max} is the maximum luminance, η_{max} indicates the maximum current efficiency, and V_T is the applied voltage for the device at luminance of 1 cd/m^2.

of devices under operation. We can see that all devices exhibit very saturated and pure red color, which completely originates from exciton recombinations in QDs. The EL peak is at λ = 610 nm with a full-width at half-maximum (fwhm) of 46 nm, similar to that of PL for QD film, peaked at λ = 603 nm and fwhm of

DOI: 10.1021/acsami.5b04050
ACS Appl. Mater. Interfaces 2015, 7, 15955−15960

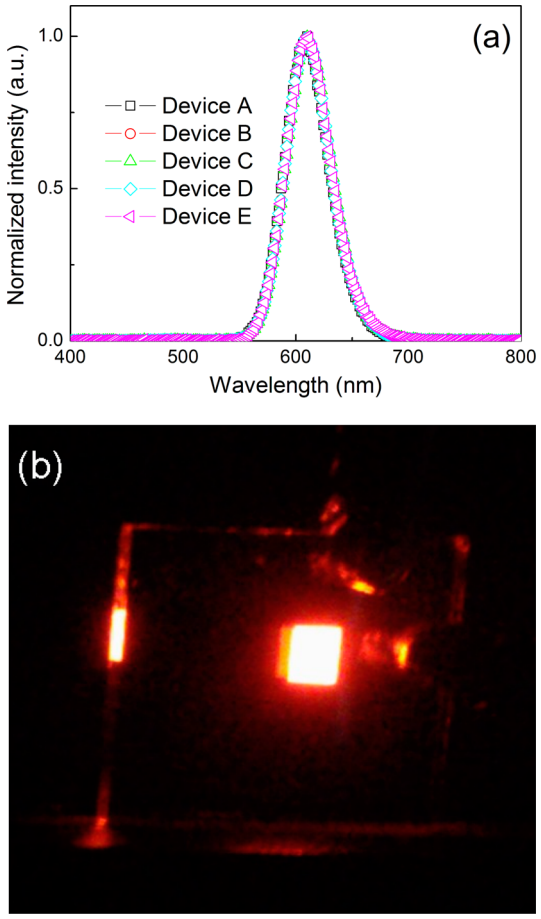

Figure 5. (a) EL spectra of QD-LEDs at voltage of 5 V; (b) photograph of device C driven under operating voltage of 4.0 V.

42 nm. All the results indicate a highly radiative recombination efficiency originating from QD band emission.

CONCLUSIONS

In summary, we fabricated highly efficient red QD-LEDs by using a stepwise HTL, and a rather high current efficiency of 16 cd/A is achieved. The stepwise HTL is composed of mCP combined with CBP as the composited structure HTL in QD-LEDs, which makes a strong charge confinement and balanced carrier injection in QDs. It is demonstrated that the mCP-containing QD-LEDs possess higher efficiency, higher brightness, and lower turn-on voltage than that of the control device with only CBP as the HTL. The low HOMO level of the hole transport material and hole mobility were dominating factors affecting QD-LED performance. The stepwise HTL plays two key roles in the devices, blocking the electron to inject into HTL due to the higher LUMO energy level of mCP and separating the exciton formation zone from the hole accumulation interface as described in our previous work.[22] In addition, the lower HOMO energy level of mCP reduces the barrier to hole injection and hence enhances the hole injection into the QDs. All in all, efficient and balanced, carrier injection/transport and strong charge confinement can be achieved by engineering the HTL, by which highly efficient QD-LEDs can be obtained to meet various applications, such as flat-panel displays and lighting systems.

ASSOCIATED CONTENT

Supporting Information

Cyclic voltammogram of CBP and mCP solved in CH_2Cl_2, TEM image of ZnO on ITO substrate, absorption and PL spectra of ZnO nanoparticles in ethonal, and AFM image of ZnO nanoparticle film on ITO substrate. The Supporting Information is available free of charge on the ACS Publications website at DOI: 10.1021/acsami.5b04050.

AUTHOR INFORMATION

Corresponding Authors

*E-mail: jiwy@ciomp.ac.cn (W.J.).
*E-mail: zhanghz@jlu.edu.cn (H.Z.).
*E-mail: zhaojl@ciomp.ac.cn (J.Z.).

Notes

The authors declare no competing financial interest.

ACKNOWLEDGMENTS

This research was supported by National Natural Science Foundation of China (Nos. 61205025, 11474131, 11274304, and 11274142) and the Jilin Province Science and Technology Research Project (20150204067GX).

REFERENCES

(1) Brus, L. E. Electron-Electron and Electron-Hole Interactions in Small Semiconductor Crystallites-the Size Dependence of the Lowest Excited Electronic State. *J. Chem. Phys.* **1984**, *80*, 4403−4409.
(2) Colvin, V. L.; Schlamp, M. C.; Alivisatos, A. P. Light-Emitting-Diodes Made from Cadmium Selenide Nanocrystals and a Semiconducting Polymer. *Nature* **1994**, *370*, 354−357.
(3) Coe, S.; Woo, W.-K.; Bawendi, M. G.; Bulović, V. Electroluminescence from Single Monolayers of Nanocrystals in Molecular Organic Devices. *Nature* **2002**, *420*, 800−803.
(4) Sun, Q. J.; Wang, Y. A.; Li, L. S.; Wang, D.; Zhu, T.; Xu, J.; Yang, C.; Li, Y. Bright, Multicoloured Light-emitting Diodes Based on Quantum Dots. *Nat. Photonics* **2007**, *1*, 717−722.
(5) Tan, Z.; Zhang, F.; Zhu, T.; Xu, J.; Wang, A. Y.; Dixon, J. D.; Li, L.; Zhang, Q.; Mohney, S. E.; Ruzyllo, J. Bright and Color-saturated Emission from Blue Light-emitting Diodes bBased on Solution-processed Colloidal Nanocrystal Quantum Dots. *Nano Lett.* **2007**, *7*, 3803−3807.
(6) Anikeeva, P. O.; Halpert, J. E.; Bawendi, M. G.; Bulović, V. Quantum Dot Light-Emitting Devices with Electroluminescence Tunable over the Entire Visible Spectrum. *Nano Lett.* **2009**, *9*, 2532−2536.
(7) Cho, K.-S.; Lee, E. K.; Joo, W.-J.; Jang, E.; Kim, T.-H.; Lee, S. J.; Kwon, S.-J.; Han, J. Y.; Kim, B.-K.; Choi, B. L.; Kim, J. M. High-performance Crosslinked Colloidal Quantum-dot Light-emitting Diodes. *Nat. Photonics* **2009**, *3*, 341−345.
(8) Kwak, J. H.; Bae, W. K.; Lee, D. G.; Park, I.; Lim, J. H.; Park, M. J.; Cho, H. D.; Woo, H. J.; Yoon, D. Y.; Char, K. H.; Lee, S. H.; Lee, C. H. Bright and Efficient Full-Color Colloidal Quantum Dot Light-Emitting Diodes Using an Inverted Device Structure. *Nano Lett.* **2012**, *12*, 2362−2366.
(9) Mashford, B. S.; Stevenson, M.; Popovic, Z.; Hamilton, C.; Zhou, Z.; Breen, C.; Steckel, J.; Bulović, V.; Bawendi, M.; Coe-Sullivan, S.; Kazlas, P. T. High-efficiency Quantum-dot Light-emitting Devices with Enhanced Charge Injection. *Nat. Photonics* **2013**, *7*, 407−412.
(10) Bae, W. K.; Park, Y.-S.; Lim, J.; Lee, D.; Padilha, L. A.; McDaniel, H.; Robel, I.; Lee, C.; Pietryga, J. M.; Klimov, V. I. Controlling the Influence of Auger Recombination on the Performance of Quantum-dot Light-emitting Diodes. *Nat. Commun.* **2013**, *4*, 2661.
(11) Shen, H.; Bai, X.; Wang, A.; Wang, H.; Qian, L.; Yang, Y.; Titov, A.; Hyvonen, J.; Zheng, Y.; Li, L. S. High-Efficient Deep-Blue Light-

DOI: 10.1021/acsami.5b04050
ACS Appl. Mater. Interfaces 2015, 7, 15955−15960

Emitting Diodes by Using High Quality $Zn_xCd_{1-x}S$/ZnS Core/Shell Quantum Dots. *Adv. Funct. Mater.* **2014**, *24*, 2367−2373.
(12) Shirasaki, Y.; Supran, G. J.; Bawendi, M. G.; Bulović, V. Emergence of Colloidal Quantum-Dot Light-Emitting Technologies. *Nat. Photonics* **2013**, *7*, 13−23.
(13) Shen, H. B.; Cao, W. R.; Shewmon, N. T.; Yang, C.; Li, L. S.; Xue, J. G. High-efficiency, Low Turn-on Voltage Blue-Violet Quantum-Dot-Based Light-Emitting Diodes. *Nano Lett.* **2015**, *15*, 1211−1216.
(14) Kim, H. H.; Park, S.; Yi, Y.; Son, D. I.; Park, C.; Hwang, D. K.; Choi, W. K. Inverted Quantum Dot Light Emitting Diodes Using Polyethylenimine Ethoxylated Modified ZnO. *Sci. Rep.* **2015**, *5*, 8968.
(15) Lim, J.; Jeong, B. G.; Park, M.; Kim, J. K.; Pietryga, J. M.; Park, Y. S.; Klimov, V. I.; Lee, C. H.; Lee, D. C.; Bae, W. K. Influence of Shell Thickness on the Performance of Light-Emitting Devices Based on CdSe/$Zn_{1-X}Cd_XS$ Core/Shell Heterostructured Quantum Dots. *Adv. Mater.* **2014**, *26*, 8034−8040.
(16) Yang, Y. X.; Zheng, Y.; Cao, W. R.; Titov, A.; Hyvonen, J.; Manders, J. R.; Xue, J. G.; Holloway, P. H.; Qian, L. High-Efficiency Light-Emitting Devices Based on Quantum Dots with Tailored Nanostructures. *Nat. Photonics* **2015**, *9*, 259−266.
(17) Dai, X. L.; Zhang, Z. X.; Jin, Y. Z.; Niu, Y.; Cao, H. J.; Liang, X. Y.; Chen, L. W.; Wang, J. P.; Peng, X. G. Solution-Processed, High-Performance Light-Emitting Diodes Based on Quantum Dots. *Nature* **2014**, *515*, 96−100.
(18) Matioli, E.; Brinkley, S.; Kelchner, K.; Hu, Y.; Nakamura, S.; DenBaars, S.; Speck, J.; Weisbuch, C. High-brightness Polarized Light emitting Diodes. *Light: Sci. Appl.* **2012**, *1*, e22.
(19) Xiang, C.; Koo, W.; So, F.; Sasabe, H.; Kido, J. A Systematic Study on Efficiency Enhancements in Phosphorescent Green, Red and Blue Microcavity Organic Light Emitting Devices. *Light: Sci. Appl.* **2013**, *2*, e74.
(20) Qian, L.; Zheng, Y.; Choudhury, K. R.; Bera, D.; So, F.; Xue, J.; Holloway, P. H. Electroluminescence from Light-emitting Polymer/ZnO Nanoparticle Heterojunctions at Sub-bandgap Voltages. *Nano Today* **2010**, *5*, 384−389.
(21) Ji, W. Y.; Jing, P. T.; Zhang, L. G.; Li, D.; Zeng, Q. H.; Qu, S. N.; Zhao, J. L. The Work Mechanism and Sub-Bandgap-Voltage Electroluminescence in Inverted Quantum Dot Light-Emitting Diodes. *Sci. Rep.* **2014**, *4*, 6974.
(22) Coe-Sullivan, S.; Steckel, J. S.; Woo, W.-K.; Bawendi, M. G.; Bulović, V. Large-area Ordered Quantum-dot Monolayers via Phase Separation during Spin-casting. *Adv. Funct. Mater.* **2005**, *15*, 1117−1124.
(23) Zhao, J.; Bardecker, J. A.; Munro, A. M.; Liu, M. S.; Niu, Y.; Ding, I.-K.; Luo, J.; Chen, B.; Jen, A. K.-Y.; Ginger, D. S. Efficient CdSe/CdS Quantum Dot Light-Emitting Diodes Using a Thermally Polymerized Hole Transport Layer. *Nano Lett.* **2006**, *6*, 463−467.
(24) Ji, W. Y.; Tian, Y.; Zeng, Q. H.; Qu, S. N.; Zhang, L. G.; Jing, P. T.; Wang, J.; Zhao, J. L. Efficient Quantum Dot Light-Emitting Diodes by Controlling the Carrier Accumulation and Exciton Formation. *ACS Appl. Mater. Interfaces* **2014**, *6*, 14001−14007.
(25) Shen, H.; Lin, Q.; Wang, H.; Qian, L.; Yang, Y.; Titov, A.; Hyvonen, J.; Zheng, Y.; Li, L. S. Efficient and Bright Colloidal Quantum Dot Light-Emitting Diodes via Controlling the Shell Thickness of Quantum Dots. *ACS Appl. Mater. Interfaces* **2013**, *5*, 12011−12016.
(26) Ji, W. Y.; Jing, P. T.; Zhao, J. L.; Liu, X.; Wang, A.; Li, H. Inverted CdSe/CdS/ZnS Quantum Dot Light Emitting Devices with Titanium Dioxide as an Electron-injection Contact. *Nanoscale* **2013**, *5*, 3474−3480.
(27) Kroger, M.; Hamwi, S.; Meyer, J.; Riedl, T.; Kowalsky, W.; Kahn, A. P-type Doping of Organic Wide Band Gap Materials by Transition Metal Oxides: A case-study on Molybdenum Trioxide. *Org. Electron.* **2009**, *10*, 932−938.
(28) Wu, M. F.; Yeh, S. J.; Chen, C. T.; Murayama, H.; Tsuboi, T.; Li, W. S.; Chao, I.; Liu, S. W.; Wang, J. K. The Quest for High-Performance Host Materials for Electrophosphorescent Blue Dopants. *Adv. Funct. Mater.* **2007**, *17*, 1887−1895.
(29) Bae, W. K.; Kwak, J.; Lim, J.; Lee, D.; Nam, M. K.; Char, K.; Lee, C.; Lee, S. Deep Blue Light-Emitting Diodes Based on $Cd_{1-x}Zn_xS$@ZnS Quantum Dots. *Nanotechnology* **2009**, *20*, 075202.
(30) Ho, M. D.; Kim, D.; Kim, N.; Cho, S. M.; Chae, H. Polymer and Small Molecule Mixture for Organic Hole Transport Layers in Quantum Dot Light-Emitting Diodes. *ACS Appl. Mater. Interfaces* **2013**, *5*, 12369−12374.

DOI: 10.1021/acsami.5b04050
ACS Appl. Mater. Interfaces 2015, 7, 15955−15960